

## Modeling multi-decadal mangrove leaf area index in response to drought along the semi-arid southern coasts of Iran



Davood Mafi-Gholami <sup>a,\*</sup>, Eric K. Zenner <sup>b</sup>, Abolfazl Jaafari <sup>c</sup>, Raymond D. Ward <sup>d,e</sup>

<sup>a</sup> Department of Forest Sciences, Faculty of Natural Resources and Earth Sciences, Shahrood University, Shahrood, Iran

<sup>b</sup> Department of Ecosystem Science and Management, The Pennsylvania State University, Forest Resources Building, University Park, PA 16802, USA

<sup>c</sup> Young Researchers and Elite Club, Karaj Branch, Islamic Azad University, Karaj, Iran

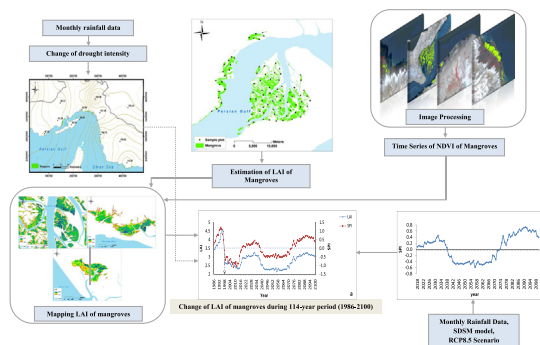
<sup>d</sup> Centre for Aquatic Environments, School of the Environment and Technology, University of Brighton, Cockcroft Building, Moulsecoomb, Brighton BN2 4GJ, United Kingdom

<sup>e</sup> Institute of Agriculture and Environmental Sciences, Estonian University of Life Sciences, Kreutzwaldi 5, EE-51014 Tartu, Estonia

### HIGHLIGHTS

- Monitoring the health of mangroves on the coasts of the Persian Gulf and the Oman Sea.
- Utilizing long-term time series of rainfall data, satellite images, and field surveys.
- Proving strong correlation between Leaf Area and Standardized Precipitation Indices.
- Predicting a sharp decrease of LAI and SPI around 2030 and increase around 2100.

### GRAPHICAL ABSTRACT



### ARTICLE INFO

#### Article history:

Received 4 September 2018

Received in revised form 29 November 2018

Accepted 30 November 2018

Available online 3 December 2018

Editor: Elena PAOLETTI

#### Keywords:

Mangroves

Health

Drought

LAI

RCP8.5

Persian Gulf

Gulf of Oman

### ABSTRACT

Leaf Area Index (LAI; as an indicator of the health) of the mangrove ecosystems on the northern coasts of the Persian Gulf and the Gulf of Oman was measured in the field and modeled in response to observed (1986–2017) and predicted (2018–2100) drought occurrences (quantified using the Standardized Precipitation Index [SPI]). The relationship of LAI with the normalized difference vegetation index (NDVI) obtained from satellite images was quantified, the LAI between 1986 and 2017 retrospectively estimated, and a relationship between LAI and SPI developed for the same period. Long-term climate data were used as input in the RCP8.5 climate change scenario to reconstruct recent and forecast future drought intensities. Both the NDVI and the SPI were strongly related with the LAI, indicating that realistic LAI values were derived from historic satellite data to portray annual changes of LAI in response to changes in SPI. Our findings show that projected future drought intensities modeled by the RCP8.5 scenario increase more and future LAIs decreased more on the coasts of the Gulf of Oman than the coasts of the Persian Gulf in the coming decades. The year 1998 was the most significant change-point for mean annual rainfall amounts and drought occurrences as well as for LAIs and at no time between 1998 and 2017 or between 2018 and 2100 are SPI and LAI values expected to return to pre-1998 values. LAI and SPI are projected to decline sharply around 2030, reach their lowest levels between 2040 and 2070, and increase and stabilize during the late decades of the 21st century at values similar to the present time. Overall, this study provides a comprehensive picture of the responses of mangroves to fluctuating future drought conditions, facilitating the development of management plans for these vulnerable habitats in the face of future climate change.

Crown Copyright © 2018 Published by Elsevier B.V. All rights reserved.

\* Corresponding author.

E-mail address: [d.mafigholami@nres.sku.ac.ir](mailto:d.mafigholami@nres.sku.ac.ir) (D. Mafi-Gholami).

## 1. Introduction

Among the natural ecological sub-systems located on the coastal areas of the world, mangroves offer a particularly diverse range of goods and services that include the provision of wood and marine products, the prevention of damage caused by storms, flood control and the protection of coastlines, control of coastal erosion, waste and pollution assimilation, recreation, and transportation (Kathiresan and Rajendran, 2005; Tamin et al., 2011; Chai et al., 2019). Despite the importance of the services mangroves provide for humans, globally >35–50% of these unique coastal habitats have already been degraded or lost over the past three decades (Valiela et al., 2001; Alongi, 2002). Whereas the severity to which mangrove ecosystems have been degraded ultimately depends on physical site-specific conditions such as the geomorphology and micro-topography, the hydro-dynamics of surface and ground water, and the sediment type of the catchment (Lewis et al., 2011; Djebou et al., 2015; Brandt et al., 2017; Xiong et al., 2018), larger scale regional factors may also contribute to declining mangrove health. For example, mangroves in the coastal areas of the Persian Gulf and the Gulf of Oman have received significant amounts of different types of pollutants during two wars in the Persian Gulf in 1988 and 1991 (Readman et al., 1996; Ebrahimi and Riahi Bakhtiari, 2010) and continue to receive industrial and municipal wastewater and >1.5 million tons of oil pollution annually, which has significantly impacted and continues to threaten their health and productivity. Finally, a substantial proportion of mangroves in the region, in particular along the western Persian Gulf (i.e., the Khamir area), continues to supply fuel wood and provide grazing opportunities for livestock (Mehrabian et al., 2009; Zahed et al., 2010).

In addition to these regional threats, climate change expressed as spatiotemporally altered rainfall/drought and ocean circulation patterns, increased average temperatures, sea levels, and storm activities has also significantly impacted, and will continue to adversely influence, the growth and health of mangroves in many parts of the world (Alongi, 2015; Ward et al., 2016; Galeano et al., 2017; Servino et al., 2018). Changes in rainfall patterns and drought occurrences are among the most important harbingers of climate change (Mishra and Singh, 2010). Lower rainfall amounts and enhanced meteorological droughts reduce the availability of freshwater and subsurface and surface runoffs, induce hydrological droughts, and increase evapotranspiration and soil salinity, which can lead to a weakening of the competitive ability of mangroves relative to adjacent communities (i.e., saltmarshes) and a reduction of current and future spatial extents/areas, productivity, and health of mangroves around the world (Gilman et al., 2008; Kovacs et al., 2009; Hutchison et al., 2014; Mafi-Gholami et al., 2017; Osland et al., 2017; Servino et al., 2018). Although mangroves are salt tolerant, decreases in freshwater inputs entering the coastal environment from upstream catchments can induce hyper-salinity in arid regions and may result in changes in the structure and function and decreased health of mangroves (Lugo et al., 1988; Ellison, 2000; Eslami-Andargoli et al., 2009; Lovelock et al., 2007; Hayes et al., 2017). It is estimated that the reduction of freshwater entering mangroves may be responsible for 11% of the global reduction in their spatial extent (Ellison and Farnsworth, 1997).

In Iran, where approximately 192 km<sup>2</sup> of mangroves exist (FAO, 2007), the extent and structure of these ecosystems exhibit a strong gradient with rainfall/drought on the northern coasts of the Persian Gulf and the Gulf of Oman and will flourish or suffer with changes in rainfall (Mafi-Gholami et al., 2017). In recent decades, mangrove ecosystems in semi-arid regions have been particularly vulnerable to increased drought occurrences and have declined drastically in spatial extent and diminished in productivity, which has largely been attributed to climate change (Eslami-Andargoli et al., 2009; Mafi-Gholami et al., 2017; Osland et al., 2017). Whereas several studies have investigated the effect of past droughts on the structure and productivity of mangroves (Eslami-Andargoli et al., 2009; Mafi-Gholami et al., 2017;

Osland et al., 2017), little is known about the magnitude of future climate-induced droughts in the region and their effects on the health of this ecosystem over the coming decades.

To quantify forest health, an appropriate indicator must be selected that should be easily understandable, be spatially and/or temporally explicit, relate to management objectives, and be quantifiable at the appropriate scale of monitoring (which can vary from trees to forest habitats) (Wicks et al., 2010; Trumbore et al., 2015; Aguirre-Rubí et al., 2018). For our purposes, the selected indicator must also be available over a long time frame and be quantifiable using remote sensing techniques because of the large spatial extent of mangroves in the study area (cf. Trumbore et al., 2015). Among the many indicators suitable for monitoring trends in forest health over time, ecological indicators that reflect biological, chemical or physical attributes such as canopy cover, total leaf area, biomass, respiration or photosynthesis have been widely used (Trumbore et al., 2015). Among these, the leaf area index (LAI) is a key biophysical variable that relates closely to the exchange of energy, water and carbon dioxide between forests and their environment (Law and Waring, 1994; Waring and Running, 1998; Clough et al., 2000; Korhonen et al., 2011) and is considered a suitable indicator of forest health (Alongi, 2002). Further, changes in LAI over time can be quantified from free or low-cost contemporary or historic satellite images that provide repeated synoptic coverages of large areas. This makes satellite imagery an effective tool for quantifying changes in the structure and health of forests (Flores-De-Santiago et al., 2013; Servino et al., 2018).

Due to their close dependency on rainfall and droughts in semi-arid regions (Mafi-Gholami et al., 2017), the fate of mangrove ecosystems in middle and lower latitudes depends on whether recent, long-term drought episodes continue in the future. If so, this would likely decrease the health and increase the rate of loss of mangroves in these regions, potentially exacerbating the anticipated adverse effects of future climate change (Solomon et al., 2007; Hutchison et al., 2014; Ellison, 2015). The main objective of this paper was to forecast the future health (quantified using the Leaf Area Index [LAI]) of the semi-arid mangroves along the northern coasts of the Persian Gulf and the Gulf of Oman in the face of likely future climate change. To achieve this objective, we developed an integrated modeling approach that combined field data with historic climate data, Landsat satellite data, and the Representative Concentration Pathway climate change scenario RCP8.5 of the fifth IPCC to reconstruct recent and forecast future droughts and mangrove health between the present time and the end of the 21st century.

## 2. Materials and methods

### 2.1. Study areas

Natural mangrove forests of Iran consist of the species Harra (*Avicennia marina*) and Chandal (*Rhizophora mucronata*). They are located on the northern coasts of the Persian Gulf and the Gulf of Oman between 25° 34' 13" N to 27° 10' 54" and 58° 34' 07" E to 55° 22' 06" E. The region enjoys a warm and humid climate (annual mean relative humidity >65%) (Mafi-Gholami et al., 2017) and receives a long-term mean annual rainfall of about 146 mm with the greatest rainfall amounts in January and February. The mean annual temperature is ~27.2 °C and ranges between 18.1 °C in the coldest month (January) and 34.5 °C in the warmest month (July). Even though mangrove forests of Iran are distributed along the majority of the northern coasts of the Persian Gulf and the Gulf of Oman, only three large areas not directly impacted by human activities were suitable for this study: Khamir, Tiab, and Jask (Fig. 1). The climate of the three studied *A. marina*-dominated mangrove forests areas is semi-arid with a mean annual precipitation of 90 mm and a relative air humidity of 35% (Pour-Asgharian, 2017).

## 2.2. Methodology framework

To predict future effects of climate change on the health of mangroves, we developed an integrated modeling approach (Supplemental Fig. 1) that combined extensive field sampling with long-term satellite imagery and climate data. We 1) sampled current (2017) LAI values in the field and derived the normalized difference vegetation index (NDVI) from concurrent Landsat satellite data, 2) developed a model to predict LAI from NDVI, 3) estimated historic, long-term (1986–2017) LAI values for which satellite, and thus NDVI, data were available, 4) established a model linking historic, long-term (1986–2017) standardized precipitation index (SPI) values that were derived from annual rainfall data as a measure of drought intensity to the estimated LAI values, 5) used the climate change scenario RCP8.5 to reproduce past (1986–2017) and predict future (2018–2100) drought intensities, and 6) used the model developed in step (4) to predict future mangrove health.

### 2.3. LAI from field sampling

LAI measurements were carried out in sample plots with an AccuPAR LP-80 Ceptometer in August and September 2017 on the same date when the most recent satellite images of the study area were captured. Measurements followed the process outlined by Kovacs et al. (2009) that was adapted for the specific conditions of mangroves (i.e., unstable sedimentary beds) and the relatively long time

required to measure the LAI with the AccuPAR LP-80. All measurements were taken below and above the canopy in direct sunlight during peak solar radiation hours. Considering that a 15-m spatial resolution of the pan-sharpened multi-spectral data is necessary for a clear separation of mangroves from its peripheral vegetation (i.e., the separation of fringe mangroves from saltmarshes), square on-the-ground sample plots with dimensions of 45 m × 45 m (area of 2025 square meters) corresponding to a 3 × 3-pixel window on the satellite image were placed throughout the study areas (Fig. 1). Distances between plot centers were 150 m (a multiple of 15 m). A total of 85 (Khamir), 65 (Tiab), and 43 (Jask) sample plots were established and the locations of the plot centers were recorded using GPS. In each sample plot, Ceptometer measurements were taken in a circular fashion from a central position at 45° intervals for a total of eight readings per plot that were later averaged.

### 2.4. NDVI data from Landsat satellite images

NDVI data were derived from Landsat satellite images (paths/row # 158/042, 159/041 and 160/041) taken at low tide in the months of August and September to (1) prevent potential bias due to phenological differences that arise from seasonal vegetation changes and to (2) avoid cloud cover that reduces the quality of the images and may prevent the detection of the features of interest. Following selection of the appropriate Landsat images, geometric and radiometric corrections were performed and images were geo-referenced to UTMWGS-1984

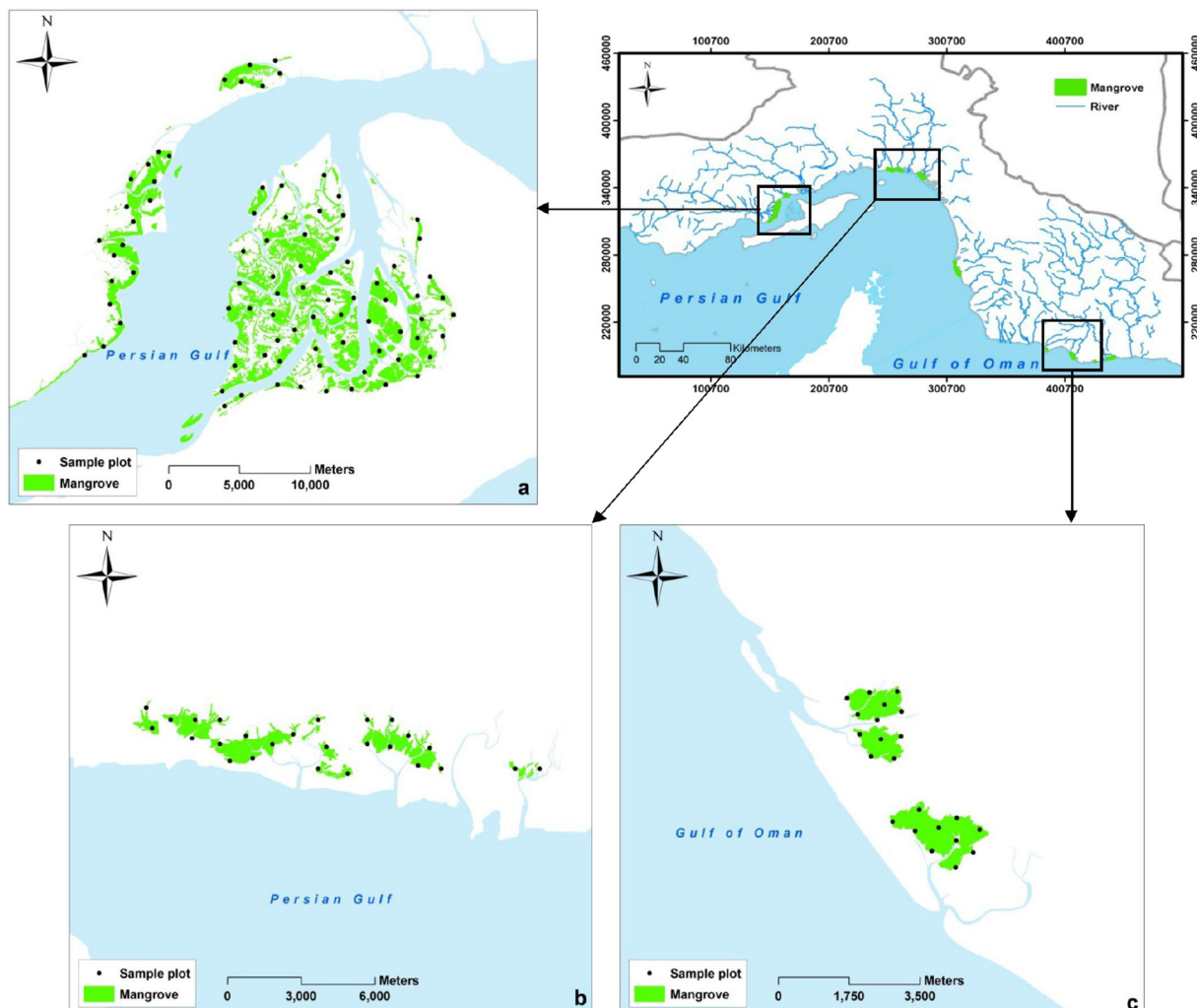


**Fig. 1.** Geographic location of the three study areas (a: Khamir, b: Tiab, c: Jask) with the sample plots (black circles).

Zone 40 N projection and datum, resulting in a root mean square error of 0.143 pixels. To minimize unimportant temporal spectral variability, the images were ortho-corrected (30 m resolution) and radiometrically normalized to a common reference image (21/09/2003) using the Multivariate Alteration Detection (MAD) method (Schroeder et al., 2006; Powell et al., 2010). To make the digital numbers (intensity values) of the pixels of each image comparable, they were converted to reflectance values. Finally, the mean normalized difference vegetation index (NDVI) values of the 9 pixels corresponding to each ground sample plot were extracted from the Landsat satellite images to develop the relationship between NDVI and LAI.

### 2.5. SPI values from recorded climate data

Based on the methods used by Mafi-Gholami et al. (2017), annual SPI values were computed for each study area using the monthly precipitation data for the 32-year measurement period between 1986 and 2017. Data were recorded at 12 meteorological stations located in the catchments and coastal areas of the three study areas and were obtained from the Iranian Meteorological Organization (IRMO). The SPI is a measure of precipitation deficit and distinguishes wet from dry periods, with more positive SPI values indicating greater wetness and more negative SPI values indicating greater drought intensities. Previous research showed that the year 1998 was the main point of overall change in drought occurrence (SPI) on the southern coasts of Iran, when SPI values changed from positive to negative values (Mafi-Gholami et al., 2017). For the period from 1998 to 2017 that exhibited consistently negative SPI values, we also computed the drought magnitude, which is defined as the positive value of the sums of the negative SPI values (Eq. 1).

$$\text{Drought Magnitude} = - \left( \sum_{j=1}^x \text{SPI}_j \right) \quad (1)$$

where  $\text{SPI}_j$  is the negative SPI values  $j$  running continuously over a period of  $x$  months.

### 2.6. Estimating recent and future SPI values with the RCP8.5 climate change scenario

We used the geographic location and the rainfall data of three selected synoptic weather stations within the three study areas as well as data from the National Center of Environmental Prediction (NCEP) as input to the general circulation model of the Canadian Earth System Model (CanESM2) to forecast future annual SPI values. The CanESM2 model is a fourth generation coupled global climate model developed by the Canadian Centre for Climate Modeling and Analysis (CCCma) of Environment and Climate Change Canada and was obtained from the website of the Canadian Climate Data and Scenarios (CCDS) (<http://cds-dscc.ec.gc.ca>). Within the CanESM2 framework, we used the 40-year time series (1965–2005) of observed rainfall data obtained from IRMO and the SDSM 5.2 model to downscale the large-scale NCEP rainfall data under the Representative Concentration Pathway (RCP) 8.5 scenario to reproduce the recent 32-year time series of annual SPI values for the period of 1986–2017 and forecast the 82-year time series of annual SPI values for the period of 2018–2100. The reproduction of recent annual SPI values from the RCP8.5 model in comparison to annual SPI values derived from actual rainfall data was used to assess the plausibility of RCP8.5 model forecasts for this study. Among a set of potential RCPs, we chose the RCP8.5 scenario, which is the most pessimistic. It assumes a future with high population growth, relatively slow income growth, and modest rates of technological change and energy intensity improvements, leading to high energy demand and GHG emissions in the long term in the absence of more stringent climate change

policies. The RCP8.5 thus corresponds to the pathway with the highest greenhouse gas emissions (Riahi et al., 2011).

### 2.7. Data analyses

Least squares regression analysis was used to develop separate functional relationships for each study area between the 2017 satellite-derived NDVI values and the field-sampled LAI values. The resulting regression models were then applied to the 32-year time series of NDVI values derived from 90 Landsat satellite images to predict corresponding LAI values for each study area. A least squares regression analysis was also used to relate the predicted LAI values to SPI values in each study area over the same observation period. The resulting regression equations were then applied to predict LAI values for each study area from the RCP8.5-predicted rainfall data/SPI values for the 114-year period between 1986 and 2100. In both cases, the regression analyses were done in the WEKA software after randomly dividing each of the two data sets into a training (2/3 of the data) and a validation (1/3 of the data) dataset (Powell et al., 2010). Splitting the datasets into a training set and a validation set enables an evaluation of the reliability of the model and a quantification of how well the models predict LAI values. To evaluate the plausibility of the RCP8.5 model, we used least squares regression analysis to relate SPI values derived from measured rainfall data to SPI values predicted from the RCP8.5 model over the period from 1986 to 2017. Finally, we used a *t*-test in the SPSS software to assess whether the year 1998 was the main change point year for the NDVI-predicted and the RCP8.5-modeled LAI values of mangroves.

## 3. Results

### 3.1. Mangrove LAI and its relation to drought

Mean ( $\pm$ SE) LAI values sampled in 2017 were  $2.65 \pm 0.31$  (range: 2.11 to 4.58) in Khamir,  $2.36 \pm 0.21$  (range: 2.05 to 4.43) in Tiab, and  $2.81 \pm 0.42$  (range: 2.21 to 4.78) in Jask. For all three study areas, least-squares regressions that used 2/3 of the observations showed that models relating LAI to NDVI were statistically significant (all  $P < 0.001$ ), with adjusted  $R^2$  values of the models of 0.87–0.93 (Table 1). Model validation with the remaining 1/3 of the data confirmed the statistical significance (all  $P < 0.001$ ) and the high reliability of the models based on adjusted  $R^2$  values of 0.85–0.91 (Fig. 2).

In all three study areas, 32-year (1986–2017) NDVI-predicted LAI values closely tracked the SPI values (Fig. 3a, and b) and resulted in statistically significant (all  $P < 0.001$ ) relationships in all three study areas, with adjusted  $R^2$  values of 0.82–0.93 (Table 2). The high reliability of the models was confirmed with the remaining 1/3 of the data: all models were statistically significant (all  $P < 0.001$ ) and had adjusted  $R^2$  values of 0.79–0.92 (Fig. 4).

Between 1986 and 1998, both the SPI and the LAI were positive and increased over the 13-year period (indicating a moderate to severe wet period associated with greater LAI values in 1998 than in 1986). In response to decreasing rainfall after 1998, SPI and LAI values declined precipitously and stayed negative over the following 19-year period

**Table 1**

Least squares regression (LSR) modeling using 2/3 of the observations to predict the 2017 leaf area index (LAI) of mangroves from the normalized difference vegetation index (NDVI) derived from 2017 Landsat satellite images.

Study area	a	b	SE	Adj- $R^2$	P value
Khamir	0.0828	0.215	9.887	0.87	<0.001
Tiab	7.139	0.493	1.139	0.89	<0.001
Jask	8.42	0.273	0.627	0.93	<0.001

a and b: slope and intercept of the regression equation.

SE: standard error of the equation.

Adj- $R^2$ : adjusted R-squared.

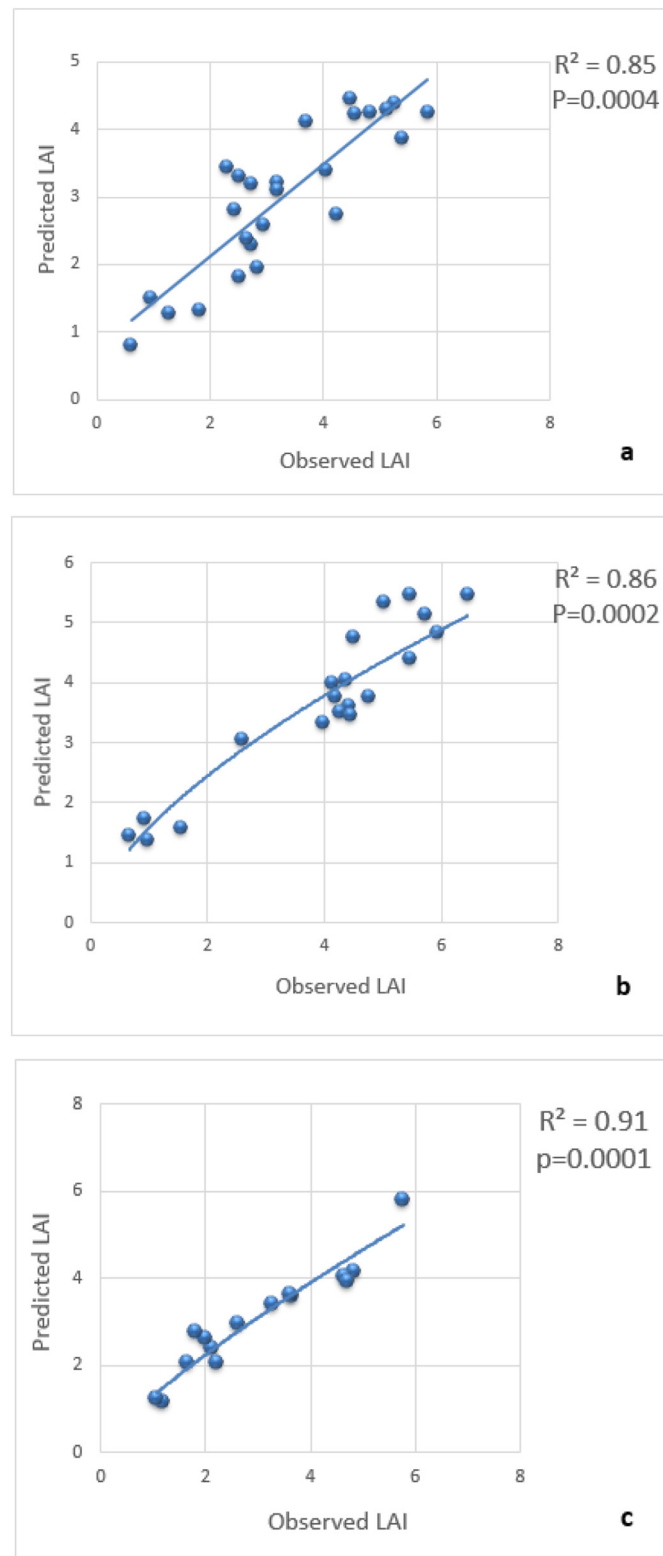


**Fig. 2.** Comparison between observed and predicted (from the normalized difference vegetation index [NDVI]) values of the leaf area index (LAI) of the validation dataset for the different study areas (a: Khamir, b: Tiab and c: Jask).

(indicating a moderate to severe dry period associated with smaller LAI values in 2017 than in 1998), with a slight reversal of this decline observed only in the last few years (Fig. 5a, b). The shift from a wet to a dry period in 1998 was reflected in the coordinated drop in LAI values

and was confirmed with *t*-tests that revealed statistically significant differences (all  $P < 0.001$ ) of mean annual LAI values before (1986–1997) and after (1998–2017) the change-point year 1998 in all three study areas.

In addition to changed mean annual LAI values before and after 1998, maximum LAI values changed substantially between the years 1986 (beginning of period), 1998 (middle of period) and 2017 (end of period) in all three study areas. For example, maximum observed LAI values in Khamir increased from 3.1 in 1986 to 3.4 in 1998 and declined to 2.6 in 2017. Similarly, maximum observed LAI values in Tiab first increased from 2.2 (1986) to 3.5 (1998) and then declined to 2.3 (2017), while in Jask these values first increased from 2.8 (1986) to 5.2 (1998) and then declined to 2.5 (2017). Fig. 5 depicts the spatial distribution of LAI values for Khamir for the years 1986, 1998, and 2017 and shows the spatial and temporal variability of increases and declines in LAI. The corresponding spatial distributions of LAI values for Tiab and Jask that showed similar temporal patterns to Khamir are shown in Supplemental Figs. (1) and (2).

In addition to the spatio-temporal within-study area variation in LAI, we also observed a regional west-east gradient in drought magnitudes (~20% difference along the gradient; Supplement Fig. 4) and severity of recent LAI reductions through time. Whereas westernmost Khamir (Persian Gulf), experienced a mean LAI reduction of 45% (from 4.5 [pre-1998] to 2.9 [post-1998]), centrally situated Tiab (located at the transition from the Persian Gulf to the Gulf of Oman) experienced a 40% LAI reduction (from 3.5 to 2.1) and easternmost Jask (Gulf of Oman) a 48% LAI reduction (from 4.3 to 2.2).

### 3.2. Predicted recent and future drought intensity and mangrove LAs from the RCP8.5 scenario

Under the RCP8.5 scenario, monthly rainfall amounts were predicted and annual SPI values were derived for the past 32-year (1986–2017) and the future 82-year (2018–2100) period. SPI values for the period of 1986–2017 projected by the RCP8.5 for each study area closely matched SPI values derived from measured rainfall amounts. Statistically significant (all  $P < 0.001$ ) regressions indicated that the RCP8.5 model was capable of reproducing plausible SPI values ( $R^2$  0.91–0.94; Supplement Fig. 5). Further, and similar to the development of the SPI derived from measured values, the RCP8.5-projected time series of SPI values correctly included the increase in wetness between 1986 and 1998, accurately portrayed the steep decline from wet to drought conditions in 1998 and shortly thereafter, and appropriately stayed at moderate drought levels between 1998 and 2017, indicating only a modest lessening of drought intensities toward the end of the period. For the future, the RCP8.5 projects increased rainfall and thus decreased drought intensities between 2018 to the mid-2030 in all study areas (Fig. 6). Beginning in the mid-2030s however, decreasing rainfall amounts and negative SPI values are projected for all three study areas. This signals the beginning of a long-term moderate drought that continues for some decades and lasts until the mid-2070s in Khamir and Tiab and the mid-2080s in Jask, with greater drought intensity projected for Jask followed by Tiab and Khamir. Finally, between the mid-2070s and 2080s, the RCP8.5 scenario projects increasing annual SPI values until the end of the 21st century. Increasing rainfall amounts are projected to end the long-term drought and result in small, positive SPI values in Khamir and Tiab, and slightly negative SPI values in Jask, indicating a continued moderate drought there.

Not surprisingly, projected values and changes over time in LAI closely tracked those of the SPI from which they were predicted. The sharp drop in SPI values after 1998 (from an overall mean of 1.2 [pre-1998] to −1.1 [post-1998]) is mirrored in the sharp decreases in the LAI values (from an overall mean of 4 [pre-1998] to 2.6 [post-1998]) in all three study areas, as is the intermittent recovery between 2010 and the 2030s, the decrease and lowest levels of both indices between the 2030s and 2060s or 2070s (to an overall mean of 2.2 for LAI and

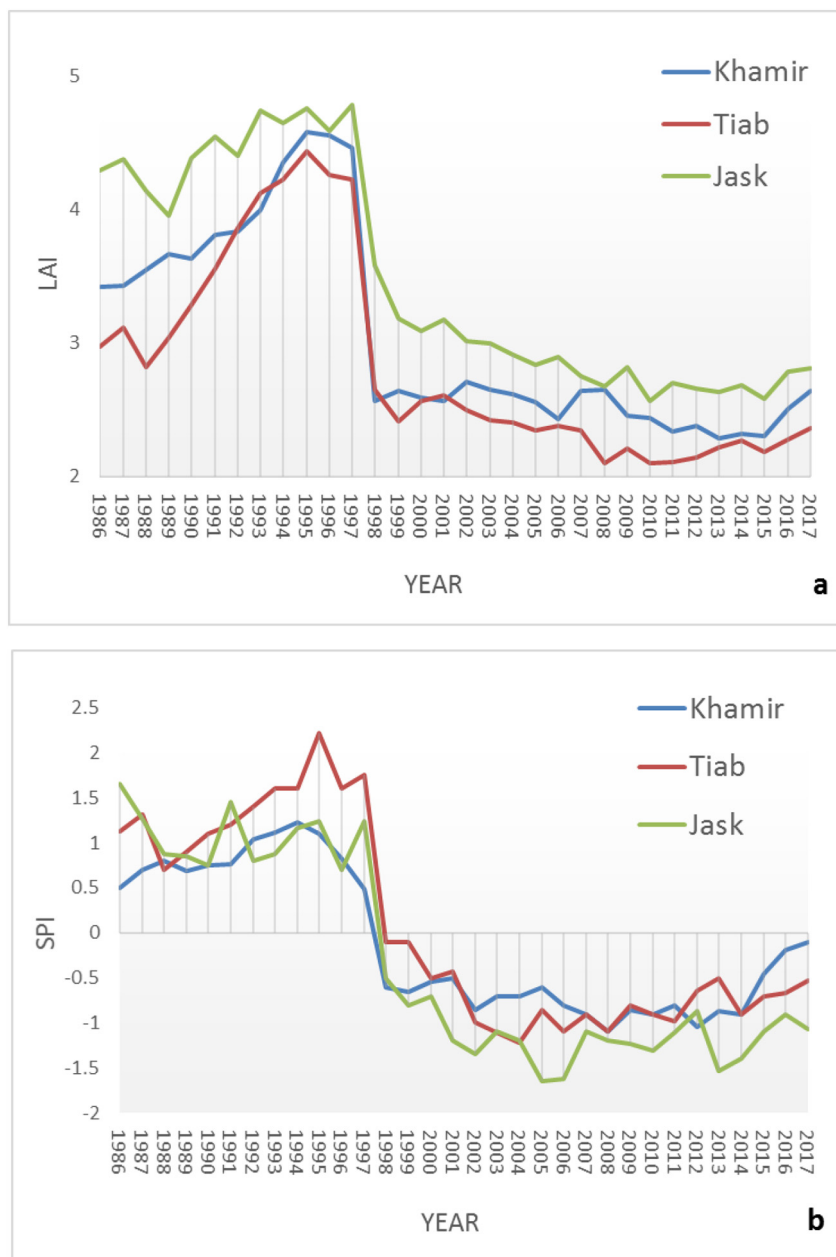


**Fig. 3.** Leaf area index (LAI) and Standardized Precipitation Index (SPI) values for each study area over a 32-year period (1986–2017) (5a: LAI, 5b: SPI).

–1 for SPI), and the recovery during the latter part of the 21st century to values similar to currently observed (Fig. 6). Based on projected drought intensities and corresponding predicted LAI values, it is likely that until the end of the 21st century neither SPI nor LAI will recover to values that were observed before 1998 (Fig. 6).

#### Table 2

Least squares regression (LSR) modeling using 2/3 of the observations to model the 1986–2017 NDVI-predicted leaf area index (LAI) of mangroves from the standardized precipitation index (SPI) derived from recorded rainfall data.

Study area	a	b	SE	Adj-r <sup>2</sup>	P value
Khamir	0.911	3.114	0.235	0.82	<0.001
Tiab	0.586	2.774	0.346	0.84	<0.001
Jask	0.696	3.681	0.292	0.93	<0.001

a and b: slope and intercept of the regression equation.

SE: standard error of the equation.

Adj-r<sup>2</sup>: adjusted R-squared.

#### 4. Discussion

Confidence in the plausibility of the predicted LAI values in response to a changing climate as a realistic gauge for future mangrove health is strongly predicated on three important assumptions: 1) that mangrove health can be inferred from LAI; 2) that the LAI in mangroves is closely coupled to the SPI such that changes in the amounts of rainfall translate into changes in LAI; and 3) that the RPC8.5 climate change scenario produces reasonable estimates of annual amounts of rainfall or values of SPI. As evidenced by the successful linkage of rainfall amounts to the LAI/health of mangroves and the subsequent accurate reproduction of recent mangrove health trends, these assumptions were sufficiently met to forecast the likely future health of mangroves through the end of the 21st century.

LAI is a biophysical parameter that is increasingly used in ecological studies (Asner et al., 2003) and has been successfully linked to health of *A. marina* in several studies. For example, whereas healthy *A. marina*

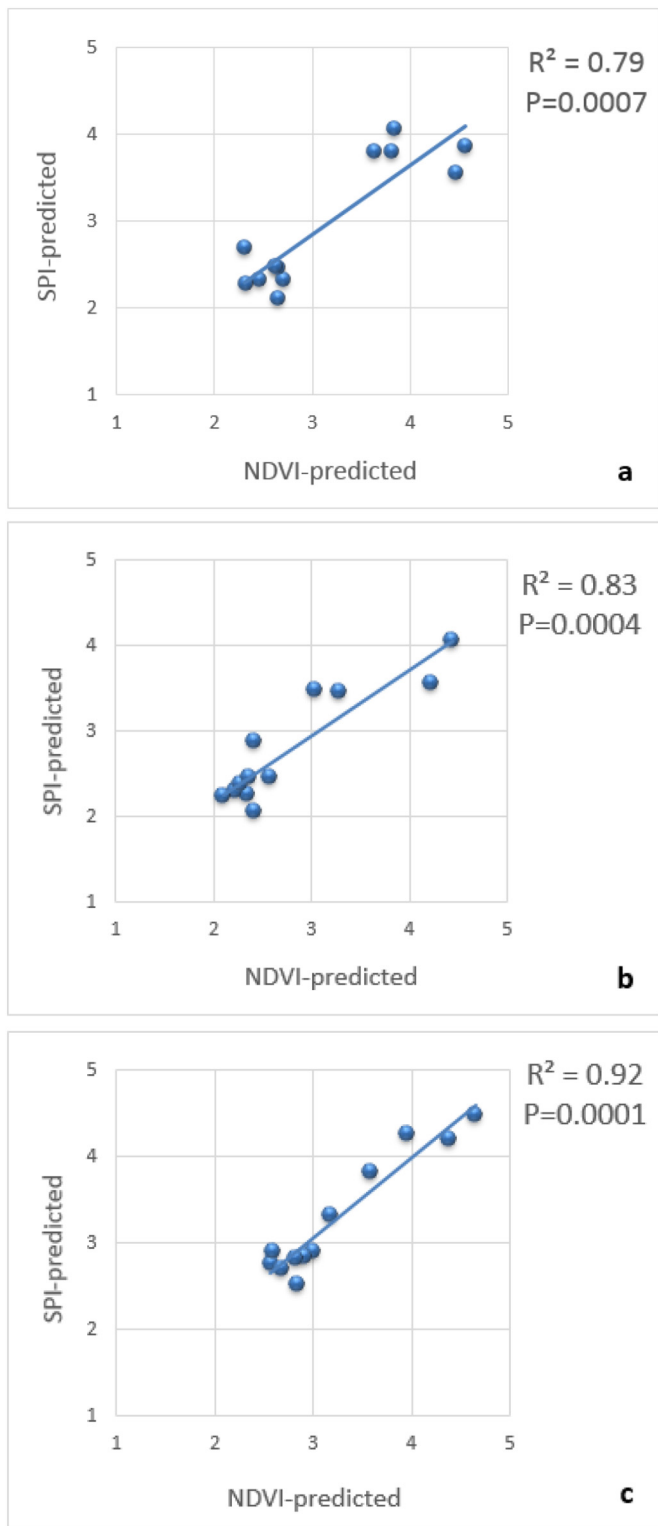


**Fig. 4.** Comparison between the normalized difference vegetation index (NDVI)-predicted and standardized precipitation index (SPI)-predicted leaf area index (LAI) values using the validation dataset of the different study areas (a: Khamir, b: Tiab and c: Jask).

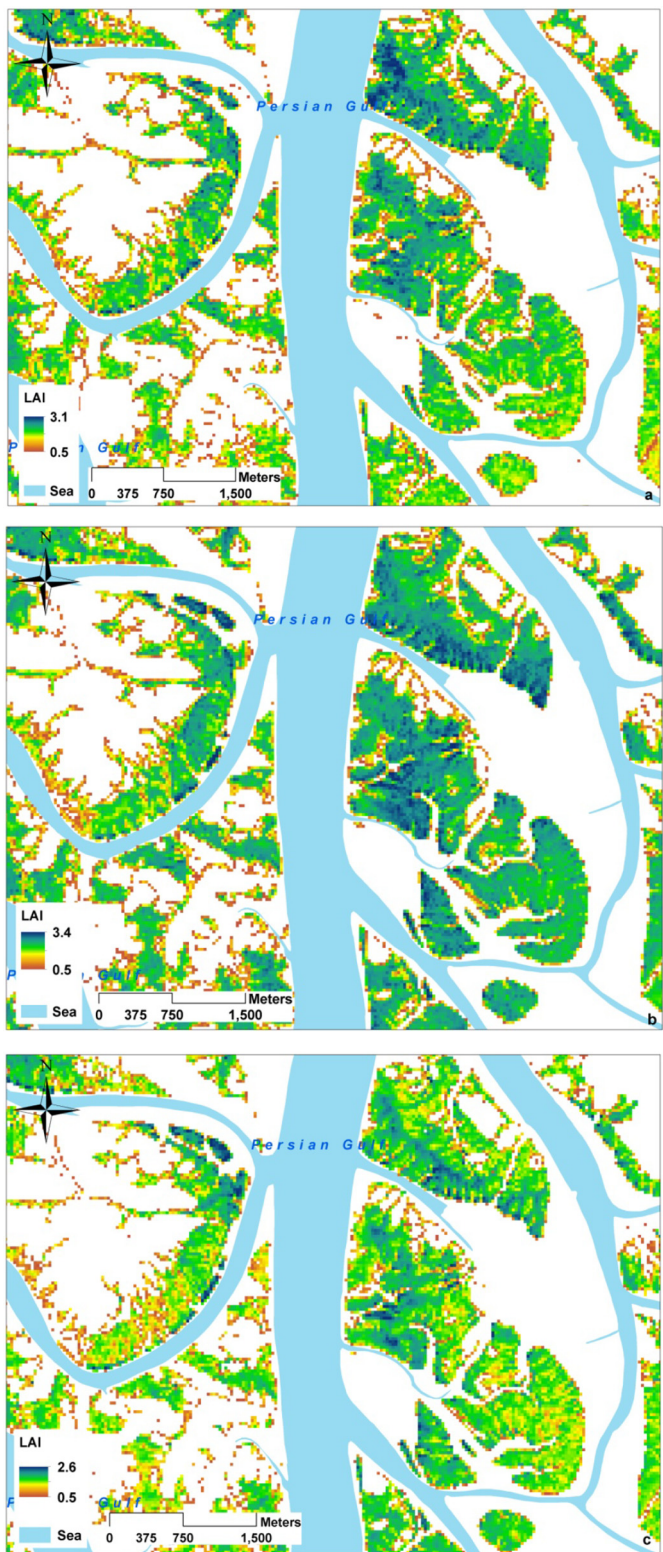


**Fig. 5.** Changes of the leaf area index (LAI) in the Khamir area through time (a: 1986; b: 1998; c: 2017).

forests in New Zealand had mean LAI values of 1.4, degraded forests had values of 1 (Lovelock et al., 2007). Similarly, healthy *A. marina* forests on semi-arid coasts of Western Australia had mean LAI values of 4 whereas degraded and lower production forests had 2.7 (Alongi et al., 2000, 2003). Finally, healthy *A. marina* forests in Thailand had mean LAI values of 3.1 whereas values in degraded forests were 1.8 (Laongmanee et al.,

2013). Although it is problematic to compare the absolute values of mangrove LAIs among different study regions because they are strongly influenced by a suite of factors such as rainfall, air temperature, wind, evapotranspiration, freshwater inflow into mangroves, nutrients, geomorphological characteristics and sedimentation dynamics, rates of sea level rise, tidal regime, storms, pollution and the structure and

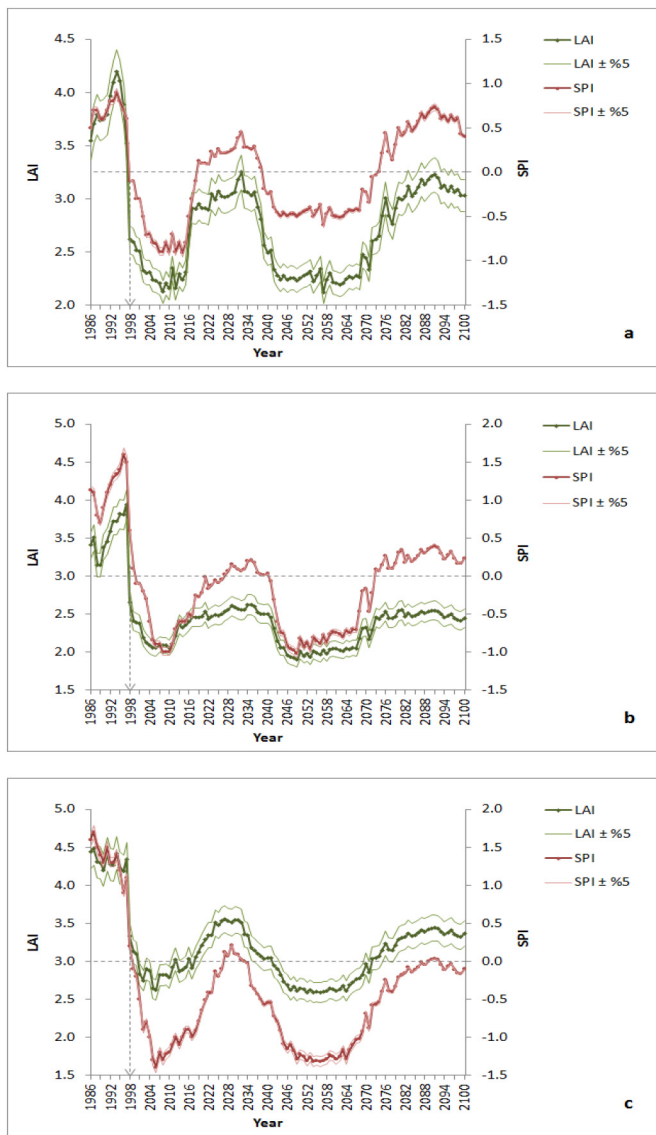


**Fig. 6.** Projected standardized precipitation index (SPI) and leaf area index (LAI) in the different study areas (a: Khamir, b: Tiab and, c: Jask) for the period between 1986 and 2100. Projected SPI values are based on the RCP8.5 climate change scenario. LAI values are predicted from regression equations developed between observed rainfall-derived SPI values and NDVI-derived LAI values for the period of 1986–2017.

composition of mangroves (Kovacs et al., 2009; Djebou et al., 2015; Brandt et al., 2017), it seems clear that declining LAI values within a study area are generally associated with declining health. Thus, LAI values in this study that declined from 3.5–4.5 before 1998 (during a comparatively wet period) to 2.1–2.9 between 1998 and 2017 provide strong evidence for a decline in mangrove health and a degradation of habitat conditions after 1998.

The temporal pattern exhibited by LAI values derived from satellite-data (i.e., NDVI) closely followed that of the SPI values derived from actual rainfall data over the most recent 32-year period, imparting confidence in our ability to forecast mangrove health from rainfall data. The SPI traced a clear climatic signal that included a steady increase in rainfall amounts, a sharp drop in rainfall amounts that induced moderate to severe droughts, a continued further gradual decline in rainfall amounts that kept the study areas in moderate or severe drought conditions for several years, and a slight recovery of rainfall that eased drought conditions in recent year. The emulation of this pattern by the LAI from satellite data obtained in the months of September and

October in response to increases and reductions in seasonal rainfall amounts of the same year indicates a close temporal coupling of these two variables. This close coupling might permit four general conclusions. First, documented adverse effects of climate change on extant mangrove ecosystems resulting in declining LAI/health may be largely driven by declining rainfall amounts (Gilman et al., 2008; Alongi, 2015; Mafi-Gholami et al., 2017). Second, mangrove ecosystems respond rapidly to changes in rainfall patterns and freshwater availability, with more adverse responses following more intense drought occurrences (Mafi-Gholami et al., 2017, 2018a, 2018b; Osland et al., 2017). Third, the deterioration of mangrove LAI/health with declining rainfall may be quickly reversible, allowing a rapid recovery of mangroves once rainfall amounts increase (Eslami-Andargoli et al., 2009). The mechanism for this rapid recovery of mangrove health is related to the water table (groundwater) recharge times and possibly nutrient delivery by surface water runoff, which tends to occur at a time scale of months and depends on soil type, vegetation community structure, rainfall and groundwater levels (Alongi, 2009). Fourth, the rapid adaptation of mangroves to the changing rainfall conditions within the same year may be a trait that enables mangroves to immediately take advantage of improved rainfall amounts or reduce stress under drought conditions. In contrast, the recovery of mangroves from other environmental stresses that induce chemical changes or physical damage seems to require more time. For example, mangroves needed about 20 years to recover from adverse effects of oil spills in coastal waters (Readman et al., 1996) and needed more than five years to recover from damages induced by a tropical cyclone (Asbridge et al., 2018).

The temporally coordinated fluctuations of the LAI/health with changes in SPI observed in this study reinforce previous findings that rainfall and drought patterns are prominent drivers of the structure (spatial extent and canopy cover) of mangroves in this semi-arid region (Mafi-Gholami et al., 2017), in the Gulf of Mexico of the United States (Bianchi et al., 2013), in Moreton Bay in Australia (Eslami-Andargoli et al., 2009), and throughout in the world (Alongi, 2015; Ellison, 2015; Osland et al., 2017; Gabler et al., 2017). These rainfall effects on mangroves were furthermore expressed by the strong spatial, west-east gradient of LAI that corresponded to the increasing drought intensity gradient from the Persian Gulf to the Gulf of Oman. This west-east gradient also coincides with a gradient in the tidal regime (average tidal ranges: Khamir 3 m; Tiab 2.3 m; Jask 1.2 m; ICZM, 2017), which directly influences the duration of inundation and soil salinity levels and thus the health, productivity, resiliency, and spatial extent of mangroves (Ellison, 2009, 2015; Hogarth, 2015). Because greater tidal ranges are associated with more variable levels of soil salinity, nutrients, and soil saturation (e.g., Sengupta and Chaudhuri, 2002; Özyurt and Ergin, 2010), the vulnerability of mangroves to rising sea levels, salinity, and inundation is lowest in westernmost Khamir (Persian Gulf) and greatest in easternmost Jask (Gulf of Oman). Although the tidal regime and rising sea levels may have amplified the observed west-east gradient in LAI responses in this study, our models indicate that rainfall/drought alone is capable of explaining much of the observed spatio-temporal variability in the LAI.

Nonetheless, despite the documented strong linkage of semi-arid mangroves and rainfall in this and other studies, mangrove ecosystems ultimately respond to changes in available freshwater amounts (Feher et al., 2017; Osland et al., 2017). While changes in upstream rainfall amounts directly affect surface and subsurface runoffs, it is actually the timing and quality of freshwater entering the coastal environment from upstream catchments that affect the structure and function of the mangroves more directly (Lugo et al., 1988; Ellison, 2000; Eslami-Andargoli et al., 2009) and ultimately determine the LAI/health of the mangroves in the region. In this study, each study area has two upstream catchments that annually deliver a significant amount of subsurface runoffs into the Persian Gulf and the Gulf of Oman during the autumn and winter seasons (Akbarian and Shayan, 2017) that maintain these mangroves in this region (Mafi-Gholami et al., 2017). With

decreasing rainfall, severe and very severe droughts (quantified using the Standardized Stream Flow Index [SSFI]) occurred in the southern parts of Iran after 1998 that resulted in a significant decline in the volume of freshwater from upstream catchments that entered the southern coastal areas (Mafi-Gholami et al., 2018a). As a consequence, the ability of rivers in the upstream catchments to maintain the spatial extent of mangroves through continued sedimentation and to maintain the health of mangroves through their moderating effects on the water salinity (Mafi-Gholami et al., 2017) may have been compromised.

Further, lower sedimentation rates following reduced rainfall and runoff may partly explain why the spatial extent of mangrove ecosystems in this region has declined in the recent past, with more severe reductions in the eastern upstream catchments on the coasts of the Gulf of Oman than the western catchments on the coasts of the Persian Gulf (Mafi-Gholami et al., 2018a). In addition to lower sedimentation rates, current relative rises in sea levels of  $1.8 \pm 0.3 \text{ mm yr}^{-1}$  indicate that mangroves are increasingly vulnerable to water inundation, which will further reduce the resiliency (i.e., to recover rapidly; Yates et al., 2014) and increase the vulnerability (i.e., to be exposed and sensitive to stresses; Ellison, 2015) of mangroves to other environmental stresses and disturbances (Gilman et al., 2007; McKee et al., 2007). Rising sea levels in the future could lead to the loss of 10 to 20% of the total area of mangroves globally (Gilman et al., 2006). Considering current rates of sedimentation and the possibility of land-migration, mangroves in our study regions are particularly vulnerable to rising sea levels, and more so along the Gulf of Oman than the Persian Gulf (Etemadi et al., 2018; Mafi-Gholami et al., 2018b), which may become an important factor for declining future mangrove health.

Simultaneously with the reduction of rainfall and the shortage of available freshwater, an increase in air temperature in the study region after 1998 also led to increased volumes of evapotranspiration that were ~6 times greater than the volume of freshwater entering the mangroves (INIOAS, 2017a). This has led to levels of salinity that exceed the tolerance of the mangrove species (Bahrami Samani et al., 2010; INIOAS, 2017b) and may be another mechanism for explaining the reduction of LAI/health after 1998. Hyper-salinization of soil pore water following increased air temperatures, drought, and shortage of freshwater has been found to result in initial decreases in seedling production, decreases in the water uptake capacity and salt exclusion, and the progressive leaf loss, branch death and finally death of *A. marina* as a result of tissue desiccation (Lovelock et al., 2007). Meanwhile, an expected increase in earth surface temperatures of ~1.4 degrees (Szulejko et al., 2017) and an increase in average annual temperature of ~3.2 °C on the southern coast of Iran (Etemadi et al., 2018) by the end of the 21st century would further increase the volume of evapotranspiration on these coasts and exacerbate the destructive effects of long-term droughts on the structure, productivity, and health of these mangroves in the coming decades.

Although our future climate projections that rely on the RCP8.5 climate change scenario preclude identifying the exact processes (i.e., changes in runoff amounts, sedimentation, hyper-salinization) that adversely or positively affect mangroves following changes in rainfall patterns in this study, we are nonetheless confident that the RCP8.5 scenario forecasts outcomes are not unrealistic. This confidence is based on the ability of the RCP8.5 scenario to accurately reproduce the distinct rainfall signals (and SPI values) that were observed between 1986 and 2017 when parameterized with past climatic data. Assuming then, that the RCP8.5 scenario is capable to accurately forecast at least the general trend of future SPI values, we find the recently observed trend of decline and recovery of SPI and LAI to continue in the future. Thus, despite predicted, continuously increasing temperatures for the region that may be ~3.2 °C (Etemadi et al., 2018) and as high as 4 °C until the end of this century under the RCP8.5 scenario (Brown and Caldeira, 2017), rainfall/drought patterns are spatially variable and do not necessarily translate into ever-increasing droughts everywhere. Although several studies have shown that the drought severity in different

regions of the world will likely increase with increasing greenhouse gas emissions and global warming over the coming decades and toward the end of the 21st century (Burke et al., 2006; McGrath et al., 2012; Dai, 2013; Trenberth et al., 2014), the regions in the mid-latitudes may be an exception that show a reduction of drought severity by the end of 21st century (Orlowsky and Seneviratne, 2013; Cook et al., 2014). Our general forecast of increasing droughts around mid-century and recovery in the last decades of the 21st century to levels similar to the present time is thus consistent with previous results and was also predicted by Zarei et al. (2016) and Gohari et al. (2017) for the Persian Gulf region. Similarly to this study, Zarei et al. (2016) and Gohari et al. (2017) expect that long-term droughts will occur on southern coast of Iran from the mid-2040s until the mid-2080s, followed by rising rainfall and reduced drought intensity by the end of the 21st century. We thus forecast that mangrove ecosystems along the Persian Gulf and the Gulf of Oman are not necessarily lost to future climate change, provided that rainfall patterns/SPI values do not drastically diverge from those forecast in this study. Nonetheless, predicted increases in sea levels with increasing temperatures poses a continued threat to mangroves in this region and might lead to future reductions in the spatial extent of these ecosystems in the Persian Gulf and the Gulf of Oman.

## 5. Conclusion

Climate change has been identified as a major cause for the decline of mangrove ecosystems around the world. Constituting the interface of terrestrial and aquatic ecosystems, mangrove forests are particularly vulnerable to the effect of climate change due to their close dependence on the supply of freshwater. Along the semi-arid southern coasts of Iran, increased frequencies and intensities of droughts might devastate currently existing mangrove ecosystems in the future. This is the first study of its kind that has used an integrated, regional-scale approach to quantify historical effects of rainfall amounts/drought intensities (SPI) on the LAI of mangroves along a spatial gradient of rainfall/drought on the northern coasts of the Persian Gulf and Gulf of Oman to forecast the future health of mangroves in response to predicted droughts under the climate change scenario RCP8.5. The RCP8.5 scenario forecasts three decades of moderate to severe droughts centered around mid-century and lesser drought intensities toward the end of the 21st century that are comparable to present time droughts for our study region. Based on the close relationship of actual SPI and LAI values observed over the most recent 32-year period in the region, we predict that the temporal trajectory of LAIs will closely track that of SPIs in the future as well. As in the past, the west-east gradient of greater drought intensity and lower LAI values from the Persian Gulf to the Gulf of Oman is expected to continue into the future. While we are confident that mangrove health is likely to worsen under drought conditions and recover whenever drought intensities lessen, our estimates of future LAI values and mangrove health status are nonetheless far from certain. In addition to the uncertainty inherent in the forecasts of long-term trends in rainfall and drought occurrences, uncertainty also arises from potential additional effects of site-specific characteristics and local environmental factors on mangrove health. These effects have generally not yet been accounted for and were assumed for this study to not change significantly in the coming decades. Because rising air temperatures and sea levels, increased human utilization for fuel and contaminants that enter mangrove ecosystems will likely weaken the health of mangroves and amplify the effects of drought in the coming decades, future studies need to more comprehensively incorporate the impacts of these other factors along with rainfall patterns and droughts to predict the long-term fate of mangrove ecosystems in the region. This methodology should also be applied in different mangrove ecosystems to better understand whether mangrove ecosystems composed of different species compositions and structures may respond to changes in rainfall and drought.

## Acknowledgment

This research did not receive any specific grant from funding agencies in the public, commercial, or not-for-profit sectors. We thank the Iranian National Institute for Oceanography and Atmospheric Science for providing the data used in this study, and four anonymous reviewers who provided many helpful comments and suggestions for improving this manuscript.

## Appendix A. Supplementary data

Supplementary data to this article can be found online at <https://doi.org/10.1016/j.scitotenv.2018.11.462>.

## References

- Aguirre-Rubí, J., Luna-Acosta, A., Ortiz-Zarragoitia, M., Zaldívar, B., Izagirre, U., Ahrens, M.J., ... Marigómez, I., 2018. Assessment of ecosystem health disturbance in mangrove-lined Caribbean coastal systems using the oyster *Crassostrea rhizophorae* as sentinel species. *Sci. Total Environ.* 618, 718–735.
- Akbarian, M., Shayan, S., 2017. Consequences of dam construction on the ecogeomorphology of coastal plains case study: coastal plains of Sedijch, Gabric and Jagin. *Hydrogeomorphology* 4 (13), 63–78 (In Persian, with English abstract).
- Alongi, D.M., 2002. Present state and future of the world's mangrove forests. *Environ. Conserv.* 29 (3), 331–349.
- Alongi, D.M., 2009. Paradigm shifts in mangrove biology. *Coastal Wetlands an Integrated Ecosystem Approach*. Elsevier, Amsterdam, Países Bajos, pp. 615–640.
- Alongi, D.M., 2015. The impact of climate change on mangrove forests. *Curr. Clim. Chang. Rep.* 1 (1), 30–39.
- Alongi, D.M., Tirindi, F., Clough, B.F., 2000. Below-ground decomposition of organic matter in forests of the mangroves *Rhizophora stylosa* and *Avicennia marina* along the arid coast of Western Australia. *Aquat. Bot.* 68 (2), 97–122.
- Alongi, D.M., Clough, B.F., Dixon, P., Tirindi, F., 2003. Nutrient partitioning and storage in arid-zone forests of the mangroves *Rhizophora stylosa* and *Avicennia marina*. *Trees* 17, 51–60.
- Asbridge, E., Lucas, R., Rogers, K., Accad, A., 2018. The extent of mangrove changes and potential for recovery following severe tropical cyclone Yasi, Hinchinbrook Island, Queensland, Australia. *Ecol. Evol.* 1–19.
- Asner, G.P., Scurlock, J.M., Hicke, A., 2003. Global synthesis of leaf area index observations: implications for ecological and remote sensing studies. *Glob. Ecol. Biogeogr.* 12 (3), 191–205.
- Bahrami Samani, L., Ebrahimi, M., Ghorbani, M., 2010. Study of horizontal and vertical distribution of physical & chemical parameters and chlorophyll in Hormoz Strait. *J. Mar. Sci. Technol.* 1–17 (In Persian, with English abstract), 3.
- Bianchi, T.S., Allison, M.A., Zhao, J., Li, X., Comeaux, R.S., Feagin, R.A., Kulawardhana, R.W., 2013. Historical reconstruction of mangrove expansion in the Gulf of Mexico: linking climate change with carbon sequestration in coastal wetlands. *Estuar. Coast. Shelf Sci.* 119, 7–16.
- Brandt, M., Tappan, G., Diouf, A.A., Beye, G., Mbow, C., Fensholt, R., 2017. Woody vegetation die off and regeneration in response to rainfall variability in the West African Sahel. *Remote Sens.* 9 (1), 39.
- Brown, P.T., Caldeira, K., 2017. Greater future global warming inferred from Earth's recent energy budget. *Nature* 552 (7683), 45.
- Burke, E.J., Brown, S.J., Christidis, N., 2006. Modeling the recent evolution of global drought and projections for the twenty-first century with the Hadley Centre climate model. *J. Hydrometeorol.* 7 (5), 1113–1125.
- Chai, M., Li, R., Shi, C., Shen, X., Li, R., Zan, Q., 2019. Contamination of polybrominated diphenyl ethers (PBDEs) in urban mangroves of southern China. *Sci. Total Environ.* 646, 390–399.
- Clough, B.F., Tan, D.T., Phuong, D.X., Buu, D.C., 2000. Canopy leaf area index and litter fall in stands of the mangrove *Rhizophora apiculata* of different age in the Mekong Delta, Vietnam. *Aquat. Bot.* 66, 311–320.
- Cook, B.I., Smerdon, J.E., Seager, R., Coats, S., 2014. Global warming and 21st century drying. *Clim. Dyn.* 43 (9–10), 2607–2627.
- Dai, A., 2013. Increasing drought under global warming in observations and models. *Nat. Clim. Chang.* 3 (1), 52.
- Djebou, D.C.S., Singh, V.P., Frauenfeld, O.W., 2015. Vegetation response to precipitation across the aridity gradient of the southwestern United States. *J. Arid Environ.* 115, 35–43.
- Ebrahimi, Z., Riahi Bakhtiari, A., 2010. Determination of oil pollution based on the determination of the concentration of polycyclic aromatic hydrocarbons (PAHs) in surface sediments of mangrove forests of Bandar Khamir coasts. The First National Conference on Technology Development in oil, gas and Petrochemical Industries. Southern Petroleum Science Institute, Ahwaz (13 p.).
- Ellison, A.M., 2000. Mangrove restoration: do we know enough? *Restor. Ecol.* 8 (3), 219–229.
- Ellison, J.C., 2009. Wetlands of the Pacific Island region. *Wetl. Ecol. Manag.* 17 (3), 169–206.
- Ellison, J.C., 2015. Vulnerability assessment of mangroves to climate change and sea-level rise impacts. *Wetl. Ecol. Manag.* 23 (2), 115–137.
- Ellison, A.M., Farnsworth, E.J., 1997. Simulated sea level change alters anatomy, physiology, growth, and reproduction of red mangrove (*Rhizophora mangle* L.). *Oecologia* 112 (4), 435–446.
- Eslami-Andargoli, L., Dale, P.E.R., Sipe, N., Chaselung, J., 2009. Mangrove expansion and rainfall patterns in Moreton Bay, southeast Queensland, Australia. *Estuar. Coast. Shelf Sci.* 85 (2), 292–298.
- Etemadi, H., Smoak, J.M., Sanders, C.J., 2018. Forest migration and carbon sources to Iranian mangrove soils. *J. Arid Environ.* 157, 57–65.
- FAO (Food and Agriculture Organization of the United Nations), 2007. The world's mangroves 1980–2005. FAO Forestry Paper. FAO, Rome, p. 153.
- Feher, L.C., Osland, M.J., Griffith, K.T., Grace, J.B., Howard, R.J., Stagg, C.L., Enwright, N.M., Krauss, K.W., Gabler, C.A., Day, R.H., Rogers, K., 2017. Linear and nonlinear effects of temperature and precipitation on ecosystem properties in tidal saline wetlands. *Ecosphere* 8 (10).
- Flores-De-Santiago, F., Kovacs, J.M., Flores-Verdugo, F., 2013. The influence of seasonality in estimating mangrove leaf chlorophyll-a content from hyperspectral data. *Wetl. Ecol. Manag.* 21 (3), 193–207.
- Gabler, C.A., Osland, M.J., Grace, J.B., Stagg, C.L., Day, R.H., Hartley, S.B., Enwright, N.M., From, A.S., McCoy, M.L., McLeod, J.L., 2017. Macroclimatic change expected to transform coastal wetland ecosystems this century. *Nat. Clim. Chang.* 7 (2), 142.
- Galeano, A., Urrego, L.E., Botero, V., Bernal, G., 2017. Mangrove resilience to climate extreme events in a Colombian Caribbean Island. *Wetl. Ecol. Manag.* 25 (6), 743–760.
- Gilman, E.L., Ellison, J., Jungblut, V., van Lavieren, H., Wilson, L., Areki, F., Brighouse, G., Bungitak, J., Dus, E., Henry, M., Kilman, M., 2006. Adapting to Pacific Island mangrove responses to sea level rise and climate change. *Clim. Res.* 32 (3), 161–176.
- Gilman, E., Ellison, J., Sauti, I., Tuamu, S., 2007. Trends in surface elevations of American Samoa mangroves. *Wetl. Ecol. Manag.* 15 (5), 391–404.
- Gilman, E.L., Ellison, J., Duke, N.C., Field, C., 2008. Threats to mangroves from climate change and adaptation options: a review. *Aquat. Bot.* 89 (2), 237–250.
- Gohari, A., Mirchi, A., Madani, K., 2017. System dynamics evaluation of climate change adaptation strategies for water resources management in Central Iran. *Water Resour. Manag.* 31 (5), 1413–1434.
- Hayes, M.A., Jesse, A., Hawke, B., Baldock, J., Tabet, B., Lockington, D., Lovelock, C.E., 2017. Dynamics of sediment carbon stocks across intertidal wetland habitats of Moreton Bay, Australia. *Glob. Chang. Biol.* 23 (10), 4222–4234.
- Hogarth, P.J., 2015. *The Biology of Mangroves and Seagrasses*. Oxford University Press.
- Hutchison, J., Manica, A., Swetnam, R., Balmford, A., Spalding, M., 2014. Predicting global patterns in mangrove forest biomass. *Conserv. Lett.* 7 (3), 233–240.
- Iranian National Institute for Oceanography and Atmospheric Science (INIOAS), 2017a. <http://www.inio.ac.ir/Default.aspx?tabid=209> (Last accessed: 21.05.2018).
- Iranian National Institute for Oceanography and Atmospheric Science (INIOAS), 2017b. <http://www.inio.ac.ir/Default.aspx?tabid=2604> (Last accessed: 11.06.2018).
- Kathiresan, K., Rajendran, N., 2005. Coastal mangrove forests mitigated tsunami. *Estuar. Coast. Shelf Sci.* 65 (3), 601–606.
- Korhonen, L., Korpela, I., Heiskanen, J., Maltamo, M., 2011. Airborne discrete-return LiDAR data in the estimation of vertical canopy cover, angular canopy closure and leaf area index. *Remote Sens. Environ.* 115 (4), 1065–1080.
- Kovacs, J.M., King, J.M.L., De Santiago, F.F., Flores-Verdugo, F., 2009. Evaluating the condition of a mangrove forest of the Mexican Pacific based on an estimated leaf area index mapping approach. *Environ. Monit. Assess.* 157 (1–4), 137–149.
- Laongmanee, W., Vaiphasa, C., Laongmanee, P., 2013. Assessment of spatial resolution in estimating leaf area index from satellite images: a case study with *Avicennia marina* plantations in Thailand. *Int. J. Geoinformatics* 9 (3).
- Law, B.E., Waring, R.H., 1994. Remote sensing of leaf area index and radiation intercepted by understory vegetation. *Ecol. Appl.* 4 (2), 272–279.
- Lewis, M., Pryor, R., Wilking, L., 2011. Fate and effects of anthropogenic chemicals in mangrove ecosystems: a review. *Environ. Pollut.* 159 (10), 2328–2346.
- Lovelock, C.E., Feller, I.C., Ellis, J., Schwarz, A.M., Hancock, N., Nichols, P., Sorrell, B., 2007. Mangrove growth in New Zealand estuaries: the role of nutrient enrichment at sites with contrasting rates of sedimentation. *Oecologia* 153 (3), 633–641.
- Lugo, A.E., Brown, S., Brinson, M.M., 1988. Forested wetlands in freshwater and salt-water environments. *Limnol. Oceanogr.* 33 (4part2), 894–909.
- Mafi-Gholami, D., Mahmoudi, B., Zener, E.K., 2017. An analysis of the relationship between drought events and mangrove changes along the northern coasts of the Persian Gulf and Oman Sea. *Estuar. Coast. Shelf Sci.* 199, 141–151.
- Mafi-Gholami, D., Baharlouii, M., Mahmoudi, B., 2018a. An investigation of the relationship between hydrological drought occurrence and mangroves areas changes. *Mar. Sci. Technol.* <https://doi.org/10.22113/jmst.2018.114535.2105> (In press). (In Persian, with English abstract).
- Mafi-Gholami, D., Baharlouii, M., Mahmoudi, B., 2018b. Investigation of climate change consequences on mangroves and saltmarshes of Hara (Avicennia Marina) biosphere reserve of Ghehsim Island. *Environ. Res.* 9 (17), 207–220 (In Persian, with English abstract).
- McGrath, G.S., Sadler, R., Fleming, K., Tregoning, P., Hinz, C., Veneklaas, E.J., 2012. Tropical cyclones and the ecohydrology of Australia's recent continental-scale drought. *Geophys. Res. Lett.* 39 (3).
- McKee, K.L., Cahoon, D.R., Feller, I.C., 2007. Caribbean mangroves adjust to rising sea level through biotic controls on change in soil elevation. *Glob. Ecol. Biogeogr.* 16 (5), 545–556.
- Mehrabian, A., Naqinezhad, A., Mahiny, A.S., Mostafavi, H., Liaghati, H., Kouchehzadeh, M., 2009. Vegetation mapping of the mond protected area of Bushehr Province (Southwest Iran). *J. Integr. Plant Biol.* 51 (3), 251–260.
- Mishra, A.K., Singh, V.P., 2010. A review of drought concepts. *J. Hydrol.* 391 (1–2), 202–216.
- Orłowsky, B., Seneviratne, S.I., 2013. Elusive drought: uncertainty in observed trends and short-and long-term CMIP5 projections. *Hydrol. Earth Syst. Sci.* 17 (5), 1765–1781.

- Osland, M.J., Feher, L.C., Griffith, K.T., Cavanaugh, K.C., Enwright, N.M., Day, R.H., Stagg, C.L., Krauss, K.W., Howard, R.J., Grace, J.B., Rogers, K., 2017. Climatic controls on the global distribution, abundance, and species richness of mangrove forests. *Ecol. Monogr.* 87 (2), 341–359.
- Özyurt, G., Ergin, A., 2010. Improving coastal vulnerability assessments to sea-level rise: a new indicator-based methodology for decision makers. *J. Coast. Res.* 265–273.
- Pour-Asgharian, A., 2017. Statistical analysis of the weather of Hormozgan province. *Q. J.* 24 (6), 17–23 (In Persian).
- Powell, S.L., Cohen, W.B., Healey, S.P., Kennedy, R.E., Moisen, G.G., Pierce, K.B., Ohmann, J.L., 2010. Quantification of live aboveground forest biomass dynamics with Landsat time-series and field inventory data: a comparison of empirical modeling approaches. *Remote Sens. Environ.* 114 (5), 1053–1068.
- Readman, J.W., Bartocci, J., Tolosa, I., Fowler, S.W., Oregioni, B., Abdulraheem, M.Y., 1996. Recovery of the coastal marine environment in the Gulf following the 1991 war-related oil spills. *Mar. Pollut. Bull.* 32 (6), 493–498.
- Raihi, K., Rao, S., Krey, V., Cho, C., Chirkov, V., Fischer, G., Kindermann, G., Nakicenovic, N., Rafaj, P., 2011. RCP 8.5 – a scenario of comparatively high greenhouse gas emissions. *Clim. Chang.* 109 (1–2), 33.
- Schroeder, T.A., Cohen, W.B., Song, C., Canty, M.J., Yang, Z., 2006. Radiometric correction of multi-temporal Landsat data for characterization of early successional forest patterns in western Oregon. *Remote Sens. Environ.* 103 (1), 16–26.
- Sengupta, A., Chaudhuri, S., 2002. Arbuscular mycorrhizal relations of mangrove plant community at the Ganges river estuary in India. *Mycorrhiza* 12 (4), 169–174.
- Servino, R.N., de Oliveira Gomes, L.E., Bernardino, A.F., 2018. Extreme weather impacts on tropical mangrove forests in the eastern Brazil marine ecoregion. *Sci. Total Environ.* 628, 233–240.
- Solomon, S., Qin, D., Manning, M., Averyt, K., Marquis, M., 2007. Climate Change 2007—the Physical Science Basis: Working Group I Contribution to the Fourth Assessment Report of the IPCC. vol. 4. Cambridge University Press.
- Szulejko, J.E., Kumar, P., Deep, A., Kim, K.H., 2017. Global warming projections to 2100 using simple CO<sub>2</sub> greenhouse gas modeling and comments on CO<sub>2</sub> climate sensitivity factor. *Atmos. Pollut. Res.* 8 (1), 136–140.
- Tamin, N.M., Zakaria, R., Hashim, R., Yin, Y., 2011. Establishment of Avicennia marina mangroves on accreting coastline at Sungai Haji Dorani, Selangor, Malaysia. *Estuar. Coast. Shelf Sci.* 94 (4), 334–342.
- Trenberth, K.E., Dai, A., van Der Schrier, G., Jones, P.D., Barichivich, J., Briffa, K.R., Sheffield, J., 2014. Global warming and changes in drought. *Nat. Clim. Chang.* 4 (1), 17.
- Trumbore, S., Brando, P., Hartmann, H., 2015. Forest health and global change. *Science* 349 (6250), 814–818.
- Valiela, I., Bowen, J.L., York, J.K., 2001. Mangrove forests: one of the world's threatened major tropical environments: at least 35% of the area of mangrove forests has been lost in the past two decades, losses that exceed those for tropical rain forests and coral reefs, two other well-known threatened environments. *AIBS Bull.* 51 (10), 807–815.
- Ward, R.D., Friess, D.A., Day, R.H., MacKenzie, R.A., 2016. Impacts of climate change on mangrove ecosystems: a region by region overview. *Ecosyst. Health Sustain.* 2 (4) e01211.
- Waring, R., Running, S., 1998. *Forest Ecosystems: Analysis at Multiple Scales*. 2nd ed. Academic Press, San Diego.
- Wicks, E.C., Longstaff, B.J., Fertig, B., Dennison, W.C., 2010. Ecological indicators-assessing ecosystem health using metrics. In: Longstaff, B.J., Carruthers, T.J.B., Dennison, W.C., Lookingbill, T.R., Hawkey, J.M., Thomas, J.E., Wicks, E.C., Woerner, J. (Eds.), *Integrating and Applying Science. A Practical Handbook for Effective Coastal Ecosystem Assessment*. Ian Press and University of Maryland Center for Environmental Science, pp. 61–77.
- Xiong, Y., Liao, B., Proffitt, E., Guan, W., Sun, Y., Wang, F., Liu, X., 2018. Soil carbon storage in mangroves is primarily controlled by soil properties: a study at Dongzhai Bay, China. *Sci. Total Environ.* 619, 1226–1235.
- Yates, K.K., Rogers, C.S., Herlan, J.J., Brooks, G.R., Smiley, N.A., Larson, R.A., 2014. Diverse coral communities in mangrove habitats suggest a novel refuge from climate change. *Biogeosciences* 11 (16), 4321–4337.
- Zahed, M.A., Rouhani, F., Mohajeri, S., Bateni, F., Mohajeri, L., 2010. An overview of Iranian mangrove ecosystems, northern part of the Persian Gulf and Oman Sea. *Acta Ecol. Sin.* 30 (4), 240–244.
- Zarei, A.R., Moghimi, M.M., Mahmoudi, M.R., 2016. Analysis of changes in spatial pattern of drought using RDI index in south of Iran. *Water Resour. Manag.* 30 (11), 3723–3743.